

# M-L band x-rays (3-3.5keV) from palladium coated targets for isochoric radiative heating of thin foil samples

Contact [bkettle01@qub.ac.uk](mailto:bkettle01@qub.ac.uk)

B. Kettle, T. Dzelzainis, S. White, M. Calvert, D. Riley

Queen's University Belfast  
University Rd, Belfast, BT7 1NN

## Introduction

The method of radiatively heating a target with a separate laser generated x-ray source is a widely used technique. Most notably this technique is used within indirect drive inertial confinement fusion (ICF) research where gold “Hohlraums” are used to heat fusible material to extremely high temperatures and densities [1]. In this text however we describe its potential use as a method for creating warm dense matter (WDM) states. Typically taken as having a solid density (1-10g/cc) and a moderate temperature (1-100eV), the properties of WDM are of great interest to many scientists, especially those concerned with the structure of matter in giant planets, where WDM conditions are thought to be common [2]. There are many aspects of WDM that can be investigated experimentally, such as the equation of state [3], the electrical and thermal conductivity, and the microscopic structure [4]. Unfortunately finding a reliable method of heating a target sample homogeneously to a WDM state, ready for probing, is not an easy task. WDM is a transient state and the sample usually requires heating as well as either compression or probing before the solid density disintegrates. This is where rapid deposition of energy is crucial. Radiative x-ray heating can fulfill this criterion. The x-ray photon energy range used for heating however has to be chosen to balance the efficiency and uniformity of energy deposition throughout the sample. Lower energy photons may be absorbed more efficiently, but will lead to preferential heating of the surface and a non-uniform sample. We investigate a viable source for isochorically heating thin foils of aluminium by studying the emission of M-L band x-rays within the 3-3.5keV range from palladium coated targets, previously detailed in Phillion et. al. [5]. We also consider the emission of lower energy radiation outside this spectral band, and its effects on sample heating.

## Experimental Setup

The experiment was conducted at VULCAN Target Area West. The experimental target setup is illustrated in figure 1. Three of the VULCAN long pulse beams were frequency doubled ( $2\omega$ ) to 526.5nm using KDP II crystals and focused onto one side of a target foil. The beams were incident at  $6^\circ$  in the horizontal plane and  $20^\circ$  degrees in the vertical plane, from target normal. Phase plates were used to give a  $250\mu\text{m}$  diameter flat top circular focal spot. Between the three beams, up to  $110\pm 5\text{J}$  in total was provided on target in 200ps Gaussian FWHM pulses. This gave an intensity of the order of  $10^{15}\text{W}/\text{cm}^2$  on target.

The targets used consisted of a thin layer of palladium coated onto a  $13.1\mu\text{m}$  CH plastic substrate. The CH substrate was on the non-irradiated side, and was designed to suppress the lower energy photons generated in the interaction. The thickness of the palladium was varied between 50nm and 400nm to observe the change in front and rear emission, with the aim to optimise L-shell emission through the rear side.

M. Notley, C. Spindloe, D. Haddock, S. Spurdle

Central Laser Facility  
Rutherford Appleton Laboratory, Didcot, OX11 0WX, UK

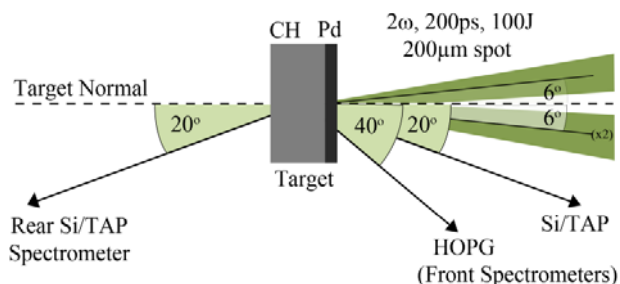


Figure 1. Experiment target setup. Laser pulses are incident from the right. They are incident  $20^\circ$  below the target normal in the vertical plane, and the beam on the lower side has another beam, incident  $20^\circ$  above the target normal.

The main diagnostics fielded to measure x-ray flux generated from the target were crystal based spectrometers. Two flat Si (111) crystals and a flat HOPG (highly ordered pyrolytic graphite) crystal were used to monitor the palladium M-L band emission in the 3-3.5keV spectral range and two flat TAP (001) crystals were used to observe radiation between 1475eV and 1550eV. This region is close to the aluminium L-edge and it is important to have an accurate grasp of the emission as aluminium is highly absorbent in this band; it will play a large role in sample heating. At this point crystal integrated reflectivities have been assumed from Henke et. al. [6]. Future work should provide a more accurate calibrated value for this variable. In each case two spectrometers observed the direct front emission, one at 20 degrees to the target normal and another at 40 degrees to the target normal. A third spectrometer observed the rear emission at 20 degrees to the target normal. Andor DX-420-BN CCD's were used as detectors on each spectrometer. Aluminium and beryllium filters were used to shield the detectors from unwanted, and potentially damaging, background radiation.

## Results

We first consider the emission detected in the 3-3.5keV range using the front and rear flat Si crystal spectrometers. Each spectrometer had  $30.4\pm 0.2\mu\text{m}$  of aluminium filtering before the crystal and  $25\mu\text{m}$  Beryllium directly before the CCD. Figure 2 (a) shows an example of a raw image from the rear Si spectrometer, along with a processed lineout (b) giving the estimated photons/sphere/eV as a function of photon energy.

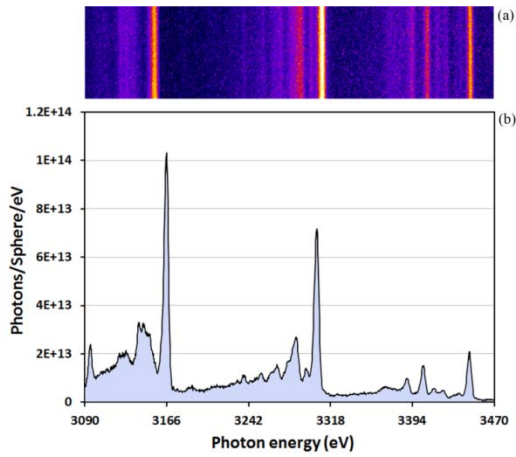


Figure 2. Sample rear Si crystal spectrometer data. Target was 50nm Pd on 13.1 $\mu$ m CH. Shot #1 15/5/2014 (a) Raw data (b) processed lineout.

We compare the total front emission (summation of all photons/sphere between 3090-3475eV) as a function of incident laser energy on target, for each shot. See figure 3.

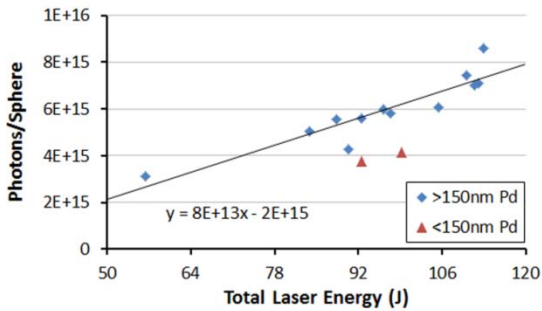


Figure 3. Total front photons/sphere emission between 3090eV-3475eV, as a function of on target laser energy (joules). Blue diamonds are targets with a palladium coating of more than 150nm. Red triangles are targets with less than 150nm of palladium coating.

There is a clear linear trend in the total flux emitted per joule of laser energy on target. Noticeable exceptions of this trend are for the cases of less than 150nm palladium coating where there is a slightly lower total yield. Figure 4 depicts the total front emission per joule as a function of palladium coating thickness.

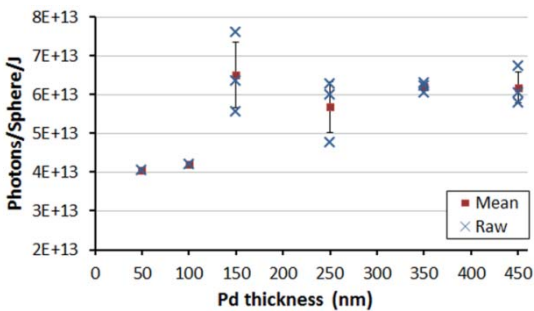


Figure 4. Total front photons/sphere emission between 3090eV-3475eV, per joule of laser energy, as a function of target palladium coating thickness. Blue crosses are raw values. Red squares are mean values. Error bars are standard deviations.

The total yield from palladium coating thicknesses between 150 to 400nm seems to be fairly consistent. However the two shots taken on thinner palladium coatings (less than 150nm), seem to be noticeably lower. This is most likely due to the heat front burning through and ablating all of the palladium, leaving a lack of material to generate x-rays. With the exception of the thinner foils, the conversion efficiency given here, approximately  $6 \times 10^{13}$  photons/sphere/joule, seems over 50% higher than the most efficient emission detailed in Phillion et. al. ( $3.78 \times 10^{13}$

photons/sphere/joule). This efficiency from Phillion also incorporates a wider photon energy bin (2.9keV-3.55keV), and should be scaled by approximately 75% to be comparable to our detected range. Possible reasons for our higher conversion efficiency than Phillion include longer laser pulse duration, higher total energy on target, or our large flat top focal spot size.

We now consider the emission in the 3-3.5keV spectral band detected by the rear Si spectrometer. The major difference here is that the x-rays have to penetrate any remaining target palladium and the 13.1 $\mu$ m CH backing. Figure 5 depicts the total rear emission per joule as a function of palladium coating thickness.

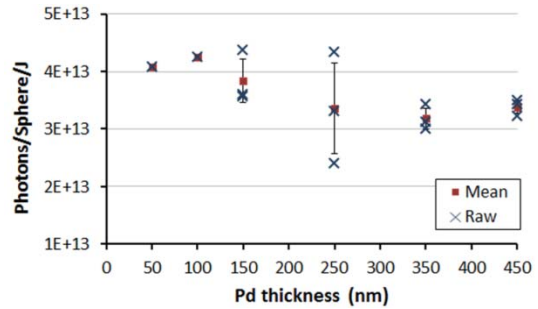


Figure 5. Total rear photons/sphere emission between 3090eV-3475eV, per joule of laser energy, as a function of target palladium coating thickness. Blue crosses are raw values. Red squares are mean values. Error bars are standard deviations.

This time the yield seems highest for thinner palladium coatings. However, in comparison to the front emission, the rear emission is still similar or lower for every case ( $4 \times 10^{13}$  photons/sphere/joule or less). Figure 6 depicts the ratio of rear total emission to front total emission. There is a prominent increase in the ratio for the two thinnest coatings. This is most likely a combination of decreased reabsorption on the rear and lower front emission for thin coatings.

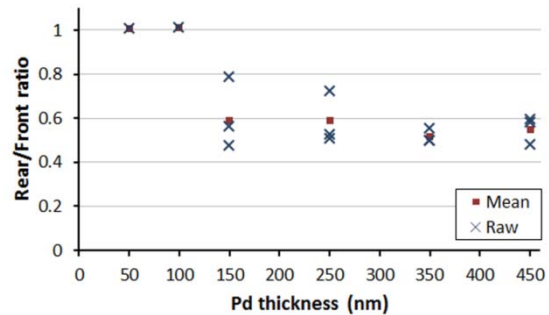


Figure 6. Ratio of rear to front total photons/sphere emission between 3090eV and 3475eV, per joule of laser energy, as a function of target palladium coating thickness. Blue crosses are raw values. Red squares are mean values.

We now consider the emission detected in the 1.5keV region with the front and rear TAP flat crystal spectrometers. The second spectrometer on the front (HOPG), verifies that the x-ray yield in the 3-3.5keV region is very similar to that of the shots with the Si spectrometers present, and it is assumed emission is comparable to shots with the Si crystal spectrometers present. Figure 7 shows an example of a raw image from the front TAP spectrometer (a) along with a processed lineout (b) giving CCD counts as a function of photon energy.

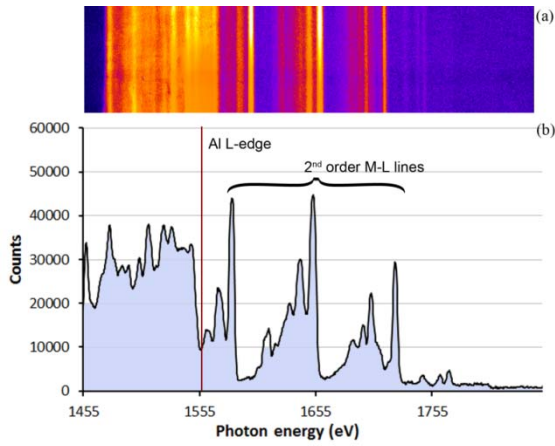


Figure 7. Sample front TAP crystal spectrometer data. Target was 150nm Pd on 13.1 $\mu$ m CH. Shot #2 9/5/2014 (a) Raw data from the CCD (b) lineout.

This time the second order M-L band 3-3.5keV lines can be seen clearly in the raw counts lineout. Before processing the data to true photon yield as a function of photon energy, the influence of the second order emission on the CCD counts on the lower side of this edge was removed. Figure 8 depicts the remaining counts between 1475eV and 1540eV, converted to photons/sphere/eV. Data from the rear TAP spectrometer is also present.

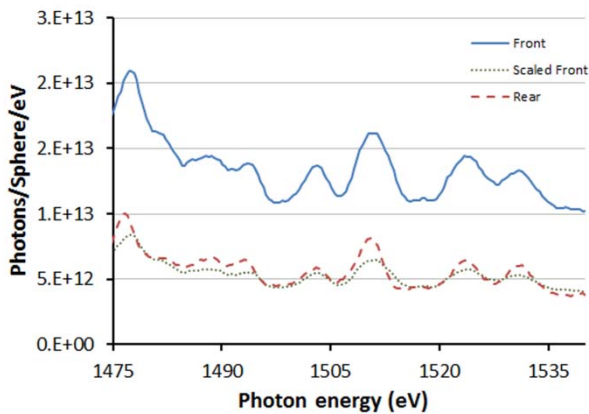


Figure 8. Total front (solid line) and rear (dashed) photons/sphere/eV between 1475 and 1540eV. Overlaid (dotted) is 40% of front values.

There seems to be quite high broadband emission within our detector region. In fact it is comparable to emission in the 3-3.5keV band from previous shots. However, the detected rear emission (dashed on figure 8) is clearly much lower than that from the front. This is due to the CH plastic backing suppressing the emission. In fact the rear yield in comparison to the front yield seems to directly follow the transmission of CH in this region (roughly 40%, dashed overlay on figure 8). We believe the broadband emission may be due to bremsstrahlung emission from within the target and that it can be spectrally modeled by a blackbody radiation fit. Thus, by assuming the radiation follows a similar temporal trend as the M-L band x-rays (200ps) and is emitted from an area of the target similar to the laser focal spot (250 $\mu$ m diameter), we match the total spectral radiance of the sample to a bulk temperature of  $\sim$ 180eV and infer a spectral profile using Planck's law. This can be used to infer emission either side of the detected band (i.e higher than the aluminium L-edge as well as lower energy photons).

### Isochorically heating thin foil aluminium

We propose the use of palladium heater targets for the heating of a thin foil aluminium sample to WDM conditions for

probing. A 0.8 $\mu$ m thick aluminium foil sample (500 $\mu$ m $\times$ 500 $\mu$ m) is simulated between two palladium foil heater targets, each 1mm from the sample. The rear emission from the palladium heater targets is taken to follow typical results outlined in the previous section. The sample is tilted at 45°, allowing a line of sight for probing and a presented area of flux for absorbing the heater x-rays. The emission from the heater foils is taken to be contained approximately within the laser focal spot area, which is divided into discrete regions, and each region is seen to emit an equally shared fraction of the total emission. The photon energy spectra emitted is approximated by various photon energy bins, and is taken to be a combination of the modeled blackbody emission, and real data from the M-L band radiation recorded with the Si spectrometers, both described previously. The sample foil is constructed of a grid of individual elements, and the flux from each heater foil emitter is in turn ray traced through the various elements of the target. Upon arrival at each element, the computed flux is absorbed according to the absorption of cold aluminium [6]. The variation in absorption of the aluminium due to photon energy is accounted for and the photon energy is assumed to be absorbed wholly by the three valence electrons of the aluminium. Figure 9 depicts the energy (eV) deposited per electron across the simulated 500 $\mu$ m $\times$ 500 $\mu$ m aluminium sample of 0.8 $\mu$ m thickness. The parameters of the simulation; 10 $\mu$ m sample X steps, 10 $\mu$ m Sample Y steps, 0.04 $\mu$ m sample Z steps, 25 $\times$ 25 grid of emitters in a 250 $\mu$ m diameter circular focal spot, 69 photon energy bins.

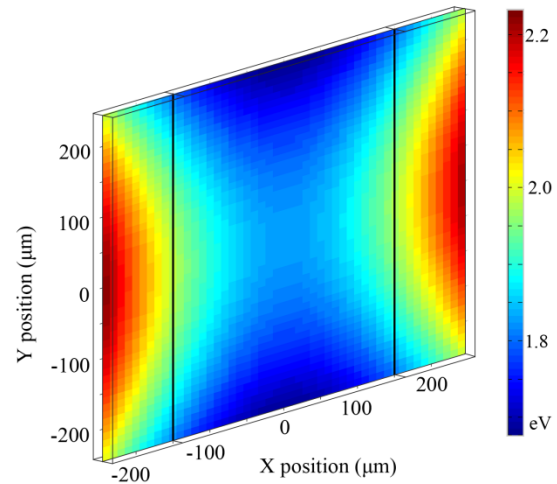


Figure 9. Lateral energy deposition (eV per valence electron) for a 0.8 $\mu$ m aluminium foil (central step), irradiated from two sides, 1mm away, using sampled emission data from palladium heater foils (including modeled blackbody emission). The black lines indicate a possible region for probing.

The variation in energy deposition across the sample is clear. At the most extreme points the sample is heated to a maximum of just over 2.2eV (at the center of the X axis edges) and a minimum of approximately 1.7eV (at the center of the Y axis edges). The non-uniformity is primarily due to the geometry of the layout (the 45° tilt of the sample foil), and the shape of the source emission (laser focal spot). This non-uniformity can be mitigated by probing only a selected lateral area of the target. The vertical black lines on figure 9 show the central 300 $\mu$ m of the sample foil. This is a large enough probe area for most diagnostics, and the energy deposition here varies between 1.7eV and 2eV, approximately a 15% variation. The distribution of energy as a function of depth through the target (Z-axis) must also be considered. Results show that along the central axis the variation is less than 0.02eV, or  $\approx$ 1%, however, at the extreme edge of the probed region the uniformity is at its

worst, and there can be a change of nearly 0.17eV,  $\approx 8\%$ . There does remain an option of tailoring the focusing geometry of the heater drive laser focal spot, to improve the uniformity of the deposition. For example, using an elliptical source should help control the deposition in the lateral direction.

The energy deposition described above is temporally integrated across the 200ps estimated duration of the x-ray source. In order to ensure a WDM state, this deposition must take place in a short enough time scale and before the sample begins to expand and the density drops. Using the results modeled in figure 9, various HYADES (a 1-D radiation hydrodynamics simulation code) [7] simulations were carried out to estimate the sample temperature and density as a function of time. We assume the energy deposition is transferred to the sample via the three valence electrons, and that it follows a temporal profile similar to that of the x-ray pulse. To that end, an electron energy source, 200ps FWHM and flat top profile, with 50ps rise/fall time was used. Although only true to the variations mentioned above, as HYADES is a 1-D simulation code, the energy deposition was taken as spatially uniform. The results of this simulation are shown in figure 10.

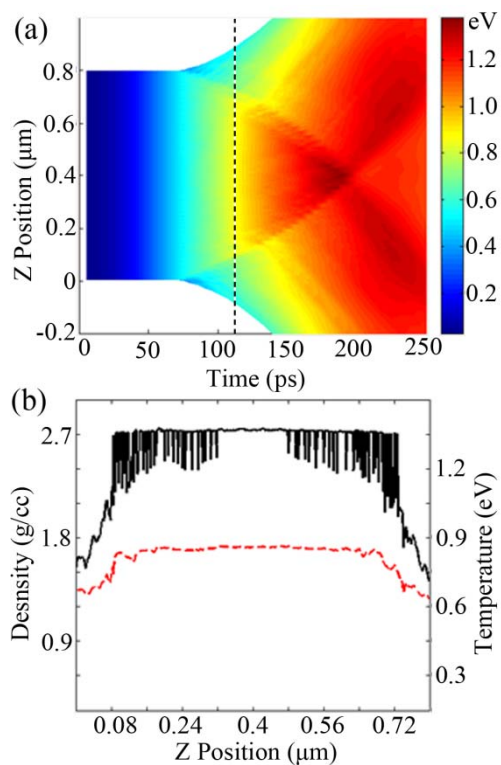


Figure 10. (a) HYADES result for the energy deposition outlined in figure 9. The vertical axis is spatial and represents the foil thickness. The horizontal axis is temporal, zero being the onset of the electron energy source. The electron temperature is given by the color bar. (b) A snapshot at 110ps. The density (solid line) and ion temperature (dotted red line) though the foil. Approximately 80% of the foil remains at solid density with a temperature of approximately nearly 0.9eV.

It can be seen that target temperature increases steadily from the onset of the heating pulse. The foil begins to expand at  $\sim 70$ ps. We take a snap shot of the sample at 110ps. See figure 10 (b). Approximately 80% of the foil remains at solid density, with a temperature of nearly 0.9eV.

## Conclusions

We have characterized the front and rear M-L band x-ray emission from various thickness palladium coated plastic heater targets, irradiated with a high energy laser pulse. We have also

measured radiation around the aluminium L-edge, and modeled emission surrounding this region. By using the plastic substrate as a means of suppressing lower energy photons, we have investigated the possibility of using the rear emission of these palladium targets as a radiative x-ray heater source. Finally, although as of yet untested for creating a WDM state, simulations show promising results for using this technique to rapidly heat a thin aluminium foil sample before expansion takes place, thus creating a WDM state for probing.

## Acknowledgements

This work was supported by the Engineering and Physical Sciences Research Council (grant number EP/1031464), and the Science and Technology Facilities Council (STFC), UK. We acknowledge the support and contribution of the Target Preparation Laboratory, Vulcan laser staff and the Engineering workshop at CLF, RAL.

## References

1. J. Lindl, *Phys. Plasmas* **2**, 3933 (1995).
2. D. Alfe, M. J. Gillan, G. D. Price, *Contemporary Physics* **48**, 63-80 (2007).
3. P. Renaudin, C. Blancard, J. Clérrouin, G. Faussurier, P. Noiret, and V. Recoules, *Phys. Rev. Lett.* **91**, 7 075002-1 (2003).
4. S. White, G. Nersisyan, B. Kettle, T.W.J. Dzelzainis, K. McKeever, C.L.S. Lewis, A. Otten, K. Siegenthaler, D. Kraus, M. Roth, T. White, G. Gregori, D.O. Gericke, R. Baggott, D.A. Chapman, K. Wunsch, J. Vorberger, D. Riley, *High Energy Density Physics* **9**, 573-577 (2013).
5. D. W. Phillion and C. J. Hailey, *Phys. Rev. A* **34**, 4886 (1986).
6. B.L. Henke, E.M. Gullikson, and J.C. Davis, *Atomic Data and Nuclear Data Tables* **54** (No.2), 181-342 (1993).
7. J. T. Larsen and S. M. Lane, *J. Quant. Spectrosc. Radiat. Transfer* **51**, 179-186 (1994).